

STRUCTURE OF NEUTRON STARS * **

JAMES LATTIMER

Department of Physics & Astronomy, State University of New York
Stony Brook, NY 11794-3800, USA

(Received October 29, 1999)

Several aspects of the structure of neutron stars are considered from theoretical and observational perspectives. Theoretical limits on the mass and radius are considered, and these are compared with new observations of isolated neutron stars and quasi-periodic oscillators (QPOs). A radius determination provides information concerning the nuclear symmetry energy and its density dependence, but does not much constrain the stiffness of the EOS, contrary to popular belief. Three analytic structure solutions are discussed which shed light on other structural aspects of neutron stars, including their moments of inertia and binding energies. Pulsar glitches may constrain the distribution of the moment of inertia inside a star and supernova neutrinos, marking the birth of a neutron star, may constrain the neutron star's binding energy.

PACS numbers: 26.60.+c, 97.60.Jd

1. Introduction and theoretical considerations

The theoretical study of the structure of neutron stars is essential if new observations of masses and radii are to lead to effective constraints on the dense matter equation of state (EOS). The long-standing inability to obtain tight limits on the EOS at supernuclear densities makes such analyses ever more important. This lecture summarizes our understanding of neutron star structure, and compares theory and observations for neutron star masses, radii, moments of inertia and binding energies.

The composition of a neutron star chiefly depends on the nature of strong interactions, which are not well understood in dense matter. The several possible models investigated [15,25] can be conveniently grouped into three

* Presented at the XXIII International School of Theoretical Physics "Recent Developments in Theory of Fundamental Interactions", Ustroń, Poland, September 15–22, 1999.

** Partially supported by the US DOE Grant DE-AC02-87ER40317.

broad categories: nonrelativistic potential models, relativistic field theoretical models, and relativistic Dirac–Brueckner–Hartree–Fock models. In each of these approaches, the presence of additional softening components such as hyperons, Bose condensates or quark matter, can be incorporated. Details of the equations of state considered in this paper are summarized in Table I.

TABLE I

Equations of State-Approaches: V=Variational, FT=Field Theoretical, DBHF=Dirac–Brueckner–Hartree–Fock, SP= Schematic Potential, SQM=Strange Quark Matter; S.I.C.=Strongly interacting components (n=neutrons, p=protons, H=hyperons, K=kaons, Q=quarks).

Symbol	Reference	Approach	S.I.C.
FP	Friedman & Pandharipande [7]	V	np
WFF(1-3)	Wiringa, Fiks & Fabrocine [40]	V	np
AP(1-3)	Akmal & Pandharipande [1]	V	np
MS(1-2)	Müller & Serot [18]	FT	np
MPA(1-2)	Müther, Prakash & Ainsworth [19]	DBHF	np
ENG	Engvik <i>et al.</i> [6]	DBHF	np
PAL(1-5)	Prakash, Ainsworth & Lattimer [24]	SP	np
GMH(1-3)	Glendenning & Moszkowski [9]	FT	npH
GS(1-2)	Glendenning & Schaffner [10]	FT	npK
PCL(1-2)	Prakash, Cooke & Lattimer [26]	FT	npHQ
SQM(1-3)	Prakash, Cooke & Lattimer [26]	SQM	Q

Fig. 1 displays the mass-radius relations for cold, catalyzed matter using these EOSs. Normal stars, those with zero density at the stellar surface, have minimum masses of about $0.1 M_{\odot}$, primarily determined by the EOS below n_s . At the minimum mass, the radii are generally in excess of 100 km. Self-bound stars have finite density (but zero pressure) at the surface, and are represented here by strange quark matter (SQM) stars, in which SQM is the ultimate ground state of matter. Such stars have no minimum mass. Valid EOSs must result in maximum masses greater than $1.4 M_{\odot}$, the lower observational limit obtained from PSR 1913+16. Uncertainties in the high-density behavior of the EOS, due to the poorly constrained many-body interactions, result in a significant uncertainty in the neutron star maximum mass, which can lie in the range from 1.4 – $2.8 M_{\odot}$. Rhoades & Ruffini [27] demonstrated that the assumption of causality and knowledge of the EOS up a fiducial density ρ_f set an upper limit to the maximum mass of a neutron star: $4.2 \sqrt{\rho_s / \rho_f} M_{\odot}$, where $\rho_s = 2.7 \cdot 10^{14} \text{ g cm}^{-3}$. A practical lower mass limit for neutron stars of $1.1 - 1.2 M_{\odot}$ follows from the minimum mass of a protoneutron star, estimated by examining a lepton-rich configuration with a low-entropy inner core of $\sim 0.6 M_{\odot}$ and a high-entropy envelope [12].

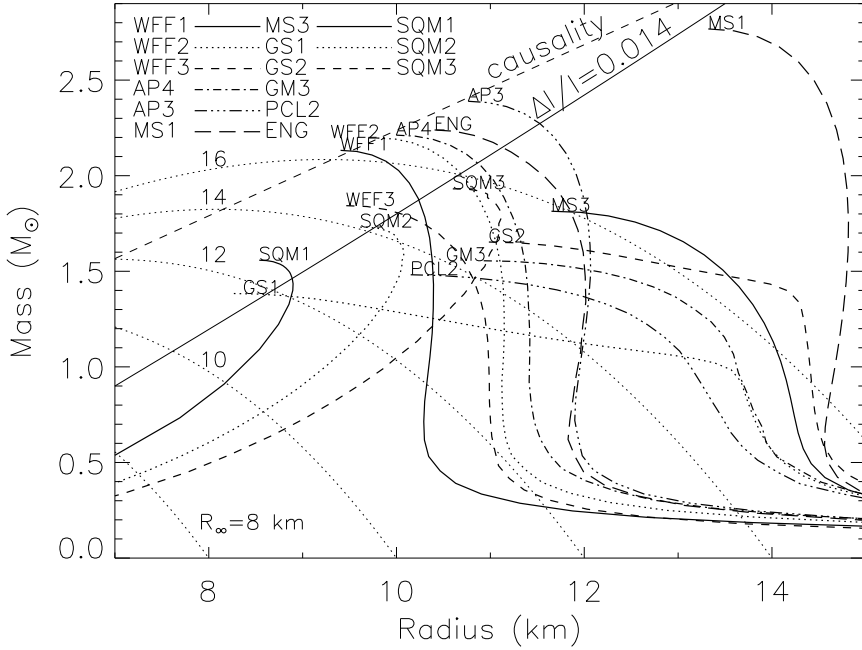


Fig. 1. $M - R$ curves for several recent EOSs listed in Table I. Contours of constant $R_\infty = R/\sqrt{1 - 2GM/Rc^2}$ are shown as dotted curves. The causal limit and the glitch constraint (Eq. 27) are shown as dashed and solid lines, respectively.

Lattimer *et al.* [15] (see also Glendenning [8]) have shown that causality also sets a lower limit to the radius: $R \gtrsim 3.04GM/Rc^2$, which is plotted in Fig. 1. In the mass range from 1 to 1.5 M_\odot or more, the radius is generally insensitive to the stellar mass. The major exception illustrated is the model GS1, in which a mixed phase containing a kaon condensate appears at a relatively low density. This leads to considerable softening and a large increase in central density for $M > 1 M_\odot$. Softening, while not as dramatic, also occurs in models GS2 and PCL2, which contain mixed phases containing a kaon condensate and strange quarks, respectively.

2. Observations of neutron star masses and radii

To date, several accurate mass determinations of neutron stars in binary radio pulsars are available [34], and they all lie in a narrow range (1.25 – 1.44 M_\odot). One neutron star in an X-ray binary, Cyg X-2, has an estimated mass of $1.8 \pm 0.2 M_\odot$ [20], but this determination is not as clean as for a radio binary. Another X-ray binary, Vela X-1, has been claimed to have a mass around 1.9 M_\odot [37], although Stickland *et al.* [33] argue it to be about 1.4 M_\odot . It would not, however, be surprising if neutron stars in

X-ray binaries had larger masses than those in radio binaries, since the latter have presumably not accreted any mass since their formation. Alternatively, Cyg X-2 could be the first of a new and rarer population of neutron stars formed with high masses which could originate from more massive, rarer, supernovae. If the high masses for Cyg X-2 or Vela X-1 are confirmed, significant constraints on the equation of state would be realized.

Unfortunately, a precise direct measurement of the radius does not yet exist. Observations from the Earth of thermal radiation from neutron star surfaces could yield values of the “radiation radius”

$$R_\infty = R/\sqrt{1 - 2GM/Rc^2}, \quad (1)$$

which results from comparison of luminosities emitted from the star’s surface $L = 4\pi R^2 \sigma T^4$ and observed at infinity $L_\infty = 4\pi R_\infty^2 \sigma T_\infty^4$ (for blackbodies). $L_\infty = L(1 - 2GM/Rc^2)$ and $T_\infty = T\sqrt{1 - 2GM/Rc^2}$ are the redshifted luminosity and temperature, respectively. Contours of R_∞ are compared with $M - R$ trajectories for several recent, representative EOSs (references and notes are listed in Table I) in Fig. 1. Values of R_∞ in the range of 12–20 km are possible for neutron stars with masses $\gtrsim 1 M_\odot$.

Estimates of neutron star radii from observations have given a wide range of results. Those pulsars with at least some suspected thermal radiation generically yield effective values of R_∞ so small that it is believed that the radiation originates from polar hot spots rather than from the surface as a whole. For example, Golden & Shearer [11] found that upper limits to the unpulsed emission from Geminga, coupled with a parallactic distance of 160 pc, yielded values of $R_\infty \lesssim 9.5$ km for a blackbody source and $R_\infty \lesssim 10$ km for a magnetized H atmosphere. Similarly, Schulz [30] estimated emission radii of less than 5 km, assuming a blackbody for eight low mass X-ray binaries. Other attempts to deduce a radius include analyses [35] of X-ray bursts from sources 4U 1705-44 and 4U 1820-30 which also implied relatively small values, $9.5 \lesssim R_\infty \lesssim 14$ km. Recently, Rutledge *et al.* [29] found that thermal emission from neutron stars of a canonical 10 km radius was indicated by the interburst emission. However, the modeling of the photospheric expansion and touchdown on the neutron star surface requires a model dependent relationship between the color and effective temperatures, rendering these estimates uncertain. Absorption lines in X-ray spectra have also been investigated [13] with a view to deducing the neutron star radius. Candidates for the matter producing the absorption lines are either the accreted matter from the companion star or the products of nuclear burning in the bursts. In the former case, the most plausible element is thought to be Fe, which would imply $R \approx 3.2GM/c^2$, only slightly larger than the causal limit. In the latter case, plausible candidates are Ti and Cr, and larger values

of the radius would be obtained. In both cases, serious difficulties remain in interpreting the large line widths, of order 100–500 eV, in the 4.1 ± 0.1 keV line observed from many sources.

A first attempt at using pulsar light curves and pulse fractions to explore the $M - R$ relation suggested relatively large radii, of order 15 km [22]. However, this method, which assumed dipolar magnetic fields, was unable to satisfactorily reconcile the calculated magnitudes of the pulse fractions and the shapes of the light curves with observations.

The discovery of Quasi-Periodic Oscillations (QPOs) from X-ray emitting neutron stars in binaries provides a possible way of limiting neutron star masses and radii. These oscillations are manifested as quasi-periodic X-ray emissions, with frequencies ranging from tens to over 1200 Hz. Some QPOs show multiple frequencies, in particular, two frequencies ν_1 and ν_2 at several hundred Hz. In the beat frequency model, the highest frequency ν_2 is associated with the Keplerian frequency ν_K of inhomogeneities or blobs in an accretion disc. The largest such frequency measured to date is $\nu_{\text{max}} = 1230$ Hz. However, general relativity predicts the existence of a maximum orbital frequency, since the inner edge of an accretion disc must remain outside of the innermost stable circular orbit at a radius of $r_s = 6GM/c^2 = 8.86(M/M_\odot)$ km, corresponding to a frequency of $\nu_K = \sqrt{GM/r_s^3}/2\pi$ (if the star is non-rotating). Equating ν_{max} with ν_K , one deduces

$$M \lesssim 1.78 M_\odot; \quad R \lesssim 15.80 \text{ km.} \quad (2)$$

The lower frequency ν_1 is associated with a beat frequency between ν_K and the spin frequency of the star [2]. This spin frequency is large enough, of order 250–350 Hz, to increase the theoretical mass limit in Eq. (2) to about $2.1 M_\odot$. This is strictly an upper limit, unless further observations support the interpretation that ν_{max} is associated with orbits at the innermost stable orbit.

However, evidence is mounting that $\nu_2 - \nu_1$ changes with time in a given source and so cannot be a rotation frequency. Osherovich & Titarchuk [21] proposed that ν_1 is the Keplerian frequency and ν_2 is a hybrid frequency of the Keplerian oscillator under the influence of a magnetospheric Coriolis force, with

$$\nu_2 = \sqrt{\nu_1^2 + (\nu/2\pi)^2}. \quad (3)$$

This relation can fit the observations. The Keplerian frequency in this model is now at most 800 Hz, leading to an upper mass limit that is nearly $3 M_\odot$ and of little practical use. An alternative model, proposed by Stella & Vietri [31], associates ν_2 with ν_K and $\nu_2 - \nu_1$ with the precession frequency of the periastron of slightly eccentric orbiting blobs at radius r in the accretion disc, so that $\nu_1 = \nu_K \sqrt{1 - 6GM/rc^2}$. Note that $(\nu_K - \nu_1)^{-1}$ is the timescale

that an orbiting blob recovers its original orientation relative to the neutron star and the Earth, so that variations in flux are expected to be observed at both frequencies ν_K and $\nu_K - \nu_1$. Presumably, even eccentricities of order 10^{-6} lead to observable effects. This model predicts that

$$\nu_1/\nu_2 = 1 - \sqrt{1 - 6(GM\nu_2)^{2/3}/c^2}, \quad (4)$$

a relation that depends only upon M . Eq. (4) agrees with observations of QPOs, but only if $1.9 \lesssim M/M_\odot \lesssim 2.1$. This result is not very sensitive to complicating effects due to stellar rotation: the Lense–Thirring effect and oblateness. This mechanism only depends on gravitometric effects, and may apply also to accreting black hole systems (Stella *et al.* 1999), lending it credence.

New prospects for a radius determination have emerged with the detection of a nearby, non-pulsing, neutron star, RX J185635-3754, in X-ray and optical radiation [38, 39]. The observed X-rays, from the ROSAT satellite, are consistent with blackbody emission with an effective temperature of about 57 eV and very little extinction. In addition, the fortuitous location of the star in the foreground of the R CrA molecular cloud limits the distance to $D < 120$ pc. The fact that the source is not observable in radio and its lack of variability in X-rays implies that it is not a pulsar unlike other identified radio-silent isolated neutron stars. This gives the hope that the observed radiation is not contaminated with non-thermal emission as is the case for pulsars. The X-ray observations of RX J185635-3754 alone yield $R_\infty/D \approx 0.06$ pc km $^{-1}$ for a best-fit blackbody. Such a value, even combined with the maximum distance of 120 pc, yields too small a value to be consistent with any neutron star with mass greater than $1 M_\odot$. But the optical flux was discovered to be about a factor of 4 brighter than the X-ray blackbody predicts. This is consistent with there being a heavy-element atmosphere [28] but not a H-dominated atmosphere [3]. The total flux is dominated by X-rays, and is proportional to the fourth power of the star’s temperature if the emission is approximately blackbody. But the optical flux, being on the Rayleigh–Jeans tail, is proportional to only the first power of the temperature. Requiring that both X-ray and optical data be matched therefore raises the estimated value of R_∞/D by a factor $4^{2/3}$; detailed atmospheric models predict a factor 3 [3]. Fig. 2 shows representative model fits to the data for various compositions. Only heavy-element (*i.e.*, pure Fe, Si, or typical results of Si-burning [“Si-ash”]) compositions give reasonable fits. The measurement of a parallax from this star could set meaningful limits to R_∞ . Another possibility is that new space-based X-ray observatories, such as Chandra or XMM, will detect line features that could pin down the atmospheric composition, M/R via the redshift, and M and R individually if the star’s gravity can be inferred.

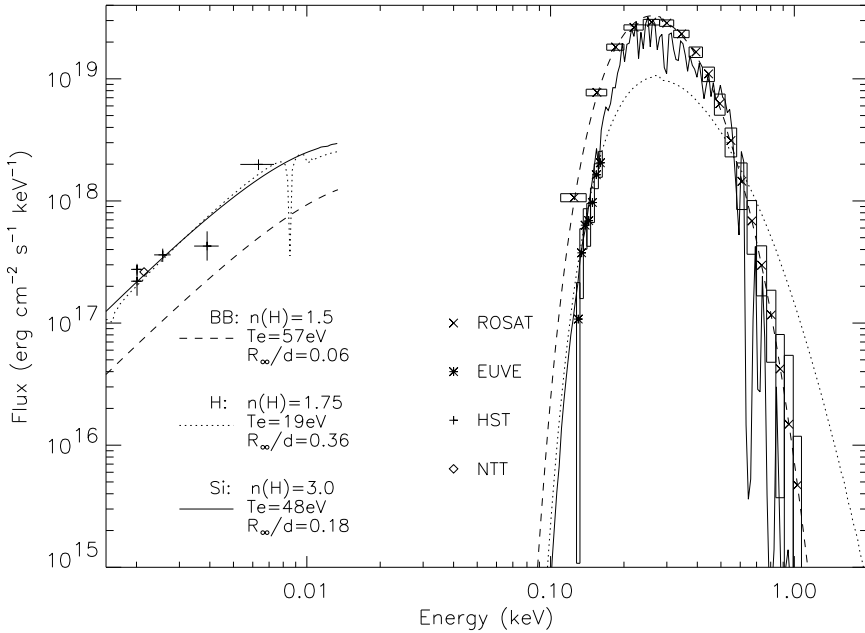


Fig. 2. Observations of RX J185635-3754 in X-rays (ROSAT), UV (EUVE) and optical (HST, NTT) radiation. Representative fits, and their parameters, for black-body (BB), hydrogen (H) and Si-ash (Si) atmosphere models are shown.

The recent discovery of an X-ray point source in the Cas A supernova remnant, presumably a neutron star formed in the explosion 320 years ago, has aroused interest. However, its large distance, 2.8 kpc, and the presence of a significant amount of interstellar absorption in the line-of-sight, about 50–100 times that towards RX J185635-3754, precludes the detection of an optical counterpart.

3. Consequences for the EOS of a radius determination

It is incorrect to state that a stiff EOS implies both a large maximum mass and a large radius. Counter examples, such as GM3 and MS3, have relatively large radii compared to most other EOSs with larger maximum masses. Nevertheless, for stars with mass greater than $1 M_{\odot}$, only models with a large degree of softening can attain $R_{\infty} < 12$ km. Should the radius of a neutron star ever be accurately determined to be this small, a strong case could be made for the existence of extreme softening at high densities.

The insensitivity of radius with mass is mimicked by a Newtonian polytrope with $n = 1$, for which R is independent of both M and the central density (ρ_c). In fact, numerical relativists have often approximated dense matter EOSs with an $n = 1$ polytrope, which also has the property that

$R \propto \sqrt{K}$, where $K = P/\rho^{1+1/n}$. This suggests that there might be a quantitative relation between the radius and the pressure at a given density that does not depend upon the EOS at higher densities, which determines the overall softness or stiffness (and hence, the maximum mass).

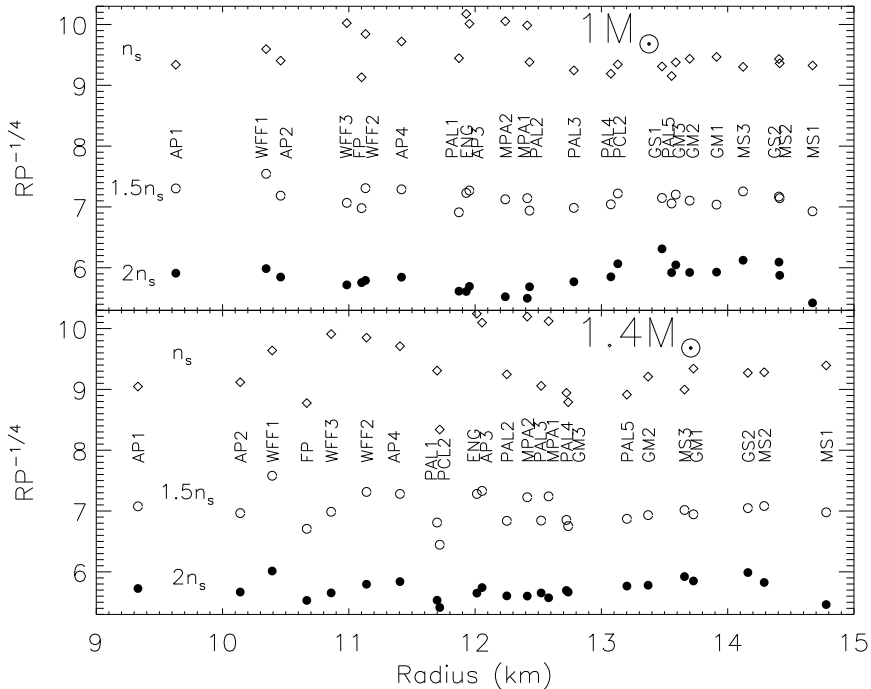


Fig. 3. Empirical relation between P , in units of MeV fm^{-3} , and R , in km, for EOSs listed in Table I. The upper panel shows results for $1 M_{\odot}$ (gravitational mass) stars; the lower panel is for $1.4 M_{\odot}$ stars. The different symbols show values of $PR^{-1/4}$ evaluated at three fiducial densities.

In fact, this conjecture is true. Fig. 3 shows the remarkable empirical correlation which exists between the radii of 1 and $1.4 M_{\odot}$ stars and the matter's pressure evaluated at fiducial densities of 1, 1.5 and $2 n_s$, where $n_s = 0.16 \text{ fm}^{-3}$. Despite the relative insensitivity of radius to mass for a particular EOS in this mass range, the nominal radius R_M , which is defined as the radius at a particular mass M in solar units, still varies widely with the EOS employed. Up to $\sim 5 \text{ km}$ differences are seen in $R_{1.4}$, for example. Of the EOSs in Table I, the only severe violation of this correlation occurs for PCL2 at $1.4 M_{\odot}$, which has extreme softening due to the existence of a mixed phase with quark matter. (Had GS1 produced a $1.4 M_{\odot}$ star, it would have violated this correlation also.) This correlation is valid only for cold, catalyzed neutron stars, *i.e.*, not for protoneutron stars which have finite entropies and possibly trapped neutrinos.

Numerically, the correlation has the form of a power law:

$$R \simeq \text{constant} [P(n)]^{0.23-0.26}, \quad (5)$$

where P is the total pressure inclusive of leptonic contributions evaluated at the density n . An exponent of $1/4$ was chosen for display in Fig. 3, but the correlation holds for a small range of exponents about this value. The correlation is marginally tighter for the baryon density $n = 1.5n_s$ and $2n_s$ cases. Note that this power is not $1/2$ as the $n = 1$ Newtonian polytrope predicts. The exponent of $1/4$ can be quantitatively understood by using a relativistic generalization of the $n = 1$ polytrope due to Buchdahl (1967). He found that the EOS

$$\rho = 12\sqrt{p_*P} - 5P, \quad (6)$$

where p_* is a constant, has an analytic solution of Einstein's equations. In this solution, R is given in terms of p_* and $\beta \equiv GM/Rc^2$ by

$$R = (1 - \beta)c^2 \sqrt{\frac{\pi}{288p_*G(1 - 2\beta)}}. \quad (7)$$

Note that R increases very slowly with β (or M) for a given value of p_* , exactly as expected from the properties of an $n = 1$ Newtonian polytrope. It is instructive to analyze the response of R to a change of pressure at some fiducial density ρ , for a fixed mass M . One finds

$$\left. \frac{d \ln R}{d \ln P} \right|_{\rho, M} = \left. \frac{d \ln R}{d \ln p_*} \right|_{\beta} \left. \frac{d \ln p_*}{d \ln P} \right|_{\rho} \left[1 + \left. \frac{d \ln R}{d \ln \beta} \right|_{p_*} \right]^{-1} \quad (8)$$

$$= \frac{1}{2} \left(1 - \frac{5}{6} \sqrt{\frac{P}{p_*}} \right) \frac{(1 - \beta)(1 - 2\beta)}{(1 - 3\beta + 3\beta^2)}. \quad (9)$$

In the limit $\beta \rightarrow 0$, one has $P \rightarrow 0$ and $d \ln R / d \ln P|_{\rho, M} \rightarrow 1/2$, the value characteristic of an $n = 1$ Newtonian polytrope. Finite values of β and P must render the exponent smaller than $1/2$. For example, if the stellar radius is about 15 km, Eq. (7) gives $Gp_*/c^4 = \pi/(288R^2) \approx 4.85 \cdot 10^{-5} \text{ km}^{-2}$. Furthermore, if the fiducial density is $\rho \approx 1.5m_b n_s \approx 2.02 \cdot 10^{-4} c^4/G \text{ km}^{-2}$ (with m_b the baryon mass), Eq. (6) implies that $GP/c^4 \approx 8.5 \cdot 10^{-6} \text{ km}^{-2}$. For $M = 1.4 M_{\odot}$, the value of β is 0.14, and one then obtains $d \ln R / d \ln P \simeq 0.31$. While this is not exactly $1/4$, the Buchdahl solution is only an approximation of realistic EOSs and provides a reasonable explanation of Eq. (5).

The existence of this correlation is significant because the pressure of degenerate neutron-star matter near n_s is primarily determined by the symmetry properties of the EOS, as we now discuss. Thus, the measurement of a neutron star radius, if not so small as to indicate extreme softening, could provide an important clue to the symmetry properties of matter. In either case, valuable information is obtained.

Studies of pure neutron matter strongly suggest that the energy of nuclear matter near n_s may be expanded in the asymmetry $(1 - 2x)$, where x is the proton fraction, and the expansion can be terminated after only one term [24]. In this case, the energy per particle and pressure of cold, beta stable nucleonic matter is

$$\begin{aligned} E(n, x) &\simeq E(n, 1/2) + S_v(n)(1 - 2x)^2, \\ P(n, x) &\simeq n^2[E'(n, 1/2) + S'_v(n)(1 - 2x)^2], \end{aligned} \quad (10)$$

where $E(n, 1/2)$ is the specific energy of symmetric matter and $S_v(n)$ is the density-dependent bulk symmetry energy. Primes denote derivatives with respect to density. At n_s , the symmetry energy can be estimated from nuclear masses and has the value $S_v \equiv S_v(n_s) \approx 27 - 36$ MeV. Attempts to further restrict this range from consideration of fission barriers and the energies of giant resonances have been ambiguous. Both the magnitude of S_v and its density dependence $S_v(n)$ are uncertain. Degenerate noninteracting nucleonic matter has a symmetry energy which is proportional to $n^{2/3}$, but interactions contribute significantly.

Leptonic contributions must to be added to Eq. (10) to obtain the total energy and pressure; the electron energy per baryon is $(3/4)\hbar c(3\pi^2 nx)^{1/3}$. Matter in neutron stars is in beta equilibrium, *i.e.*, $\mu_e = \mu_n - \mu_p = -\partial E/\partial x$, so the electronic contributions may be eliminated to cast the total pressure P at a particular density in terms of fundamental nuclear parameters. The pressure at n_s is simply

$$P_s = n_s(1 - 2x_s)[n_s S'_v(n_s)(1 - 2x_s) + S_v x_s], \quad (11)$$

where the equilibrium proton fraction at n_s is

$$x_s \simeq (3\pi^2 n_s)^{-1}(4S_v/\hbar c)^3 \simeq 0.04, \quad (12)$$

for $S_v = 30$ MeV. Due to the small value of x_s , we find that $P_s \simeq n_s S'_v(n_s)$.

Were we to evaluate the pressure at a larger density, other nuclear parameters, including the nuclear incompressibility $K_s = 9(dP/dn)|_{n_s}$ and the skewness $K'_s = -27n_s^3(d^3E/dn^3)|_{n_s}$ also become significant. For analytical purposes, the nuclear matter energy per baryon, in MeV, may be approximated in the vicinity of n_s as

$$E(n, 1/2) = -16 + \frac{K_s}{18} \left(\frac{n}{n_s} - 1 \right)^2 - \frac{K'_s}{162} \left(\frac{n}{n_s} - 1 \right)^3. \quad (13)$$

Experimental limits to the compression modulus K_s , most importantly from analyses of giant monopole resonances [4, 41] give $K_s \cong 220$ MeV. From the scaling model of the nucleus, Pearson [23] found the skewness parameter K'_s to lie in the range 1500–2500 MeV, but he neglected contributions from the surface symmetry energy. For skewnesses this large, Eq. (13) cannot be used beyond $1.5n_s$. Nevertheless, evaluating the pressure for $n = 1.5n_s$, we find

$$P(1.5n_s) = 2.25n_s [K_s/18 - K'_s/216 + n_s(1 - 2x)^2 S'_V]. \quad (14)$$

The K_s and K'_s terms nearly cancel, so that the symmetry term still comprises most of the total.

At present, experimental guidance concerning the density dependence of the symmetry energy is limited and mostly based upon the division of the nuclear symmetry energy between volume and surface contributions. Upcoming experiments involving heavy-ion collisions, which might sample densities up to $\sim (3 - 4)n_s$, will be limited to analyzing properties of the nearly symmetric nuclear matter EOS through a study of matter, momentum, and energy flow of nucleons. Thus, studies of heavy nuclei far off the neutron drip lines will be necessary in order to pin down the properties of the neutron-rich regimes encountered in neutron stars.

4. Constraints from moments of inertia and binding energies

Besides the stellar radius, other global attributes of neutron stars are potentially observable, including the moment of inertia and the binding energy. These quantities depend primarily upon the ratio M/R as opposed to details of the EOS, as can be readily seen by evaluating them using analytic solutions to Einstein's equations. There are three analytic solutions of particular interest: 1) the Schwarzschild interior solution for an incompressible fluid ("Inc"), $\rho = \rho_c$, where ρ is the mass-energy density; 2) the Buchdahl [5] solution ("Buch") described above; and 3) Tolman's [36] VII solution ("T VII"), in which the density profile is $\rho = \rho_c[1 - (r/R)^2]$.

The moment of inertia, which, for a star uniformly rotating with angular velocity Ω , is

$$I = (8\pi/3) \int_0^R r^4 (\rho + P/c^2) e^{(\lambda-\nu)/2} (\omega/\Omega) dr. \quad (15)$$

Here, the metric functions $e^\lambda \equiv g_{rr}$ and $e^\nu \equiv g_{tt}$. The metric function ω is a solution of the equation

$$\frac{d}{dr} \left[r^4 e^{-(\lambda+\nu)/2} \frac{d\omega}{dr} \right] + 4r^3 \omega \frac{d}{dr} e^{-(\lambda+\nu)/2} = 0 \quad (16)$$

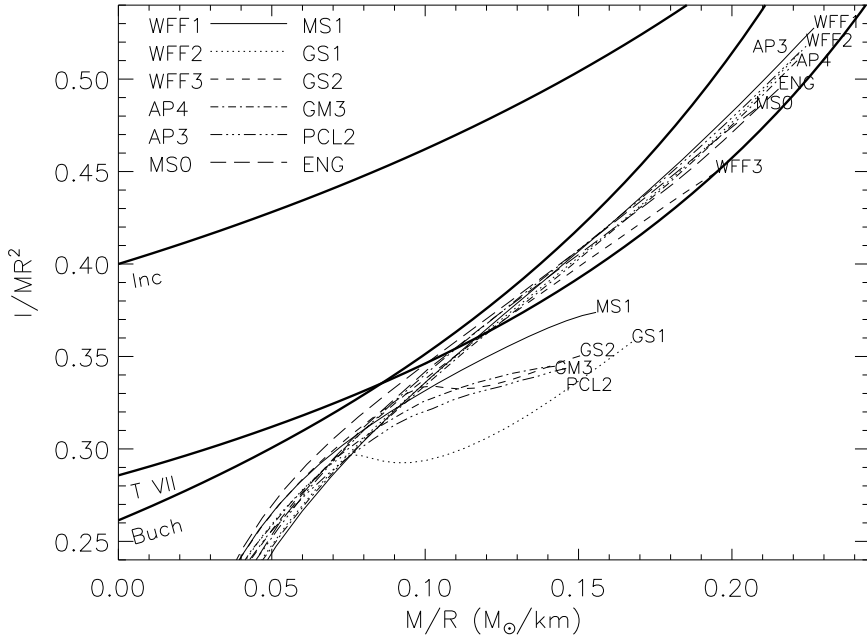


Fig. 4. The moment of inertia I , in units of MR^2 , for several EOSs listed in Table I, and for three analytic solutions of Einstein's equations.

with the surface boundary condition

$$\omega_R = \Omega - \frac{R}{3} \frac{d\omega}{dr} \Big|_R = \Omega \left[1 - \frac{2GI}{R^3 c^2} \right]. \quad (17)$$

Unfortunately, an analytic representation of ω or the moment of inertia for any of the three exact solutions is not available. However, approximations which are valid to within 0.5% are [14]

$$I_{Inc}/MR^2 \simeq 2(1 - 0.87\beta - 0.3\beta^2)^{-1}/5, \quad (18)$$

$$I_{Buch}/MR^2 \simeq (2/3 - 4/\pi^2)(1 - 1.81\beta + 0.47\beta^2)^{-1}, \quad (19)$$

$$I_{TVII}/MR^2 \simeq 2(1 - 1.1\beta - 0.6\beta^2)^{-1}/7. \quad (20)$$

In each case, the small β limit reduces to the Newtonian results. Fig. 4 compares these approximations with several recent EOSs (see Table I for details), and indicates that the Tolman VII approximation is especially good, except for very soft EOSs.

The binding energy formally represents the energy gained by assembling N baryons. If the baryon mass is m_b , the binding energy is simply $BE = Nm_b - M$ in mass units. However, the quantity m_b has various interpretations in the literature. Some authors assume it is about $940 \text{ MeV}/c^2$,

the same as the neutron or proton mass. Others assume it is about 930 MeV/ c^2 , corresponding to the mass of $C^{12}/12$ or $Fe^{56}/56$. The latter would yield the energy released in a supernova explosion and represents the energy released by the collapse of a white-dwarf-like iron core, which itself is already considerably bound. The difference, 10 MeV per baryon, corresponds to a shift of $10/940 \simeq 0.01$ in the value of BE/M . In any case, the binding energy is directly observable from the detection of neutrinos from a supernova event; indeed, it might be the most precisely determined aspect.

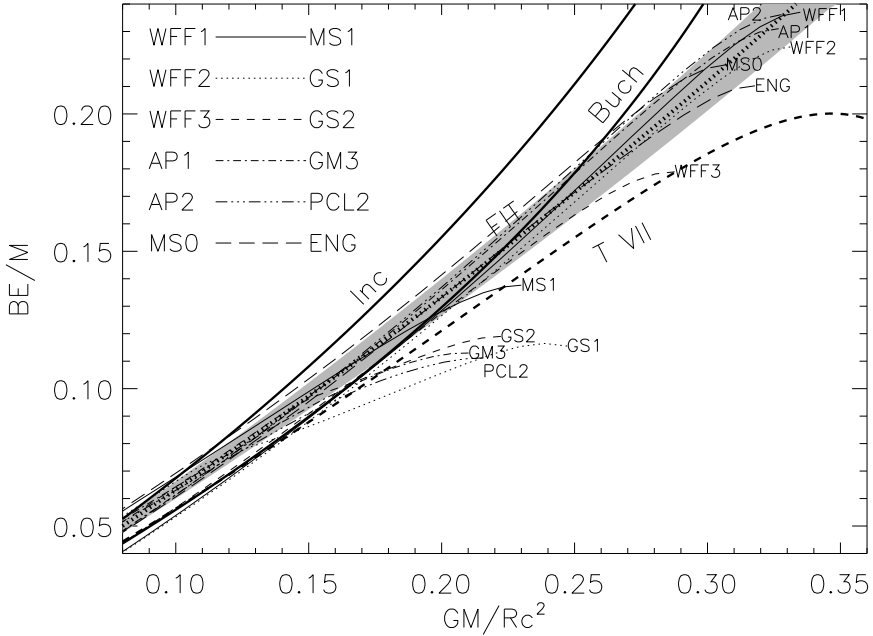


Fig. 5. The binding energy per unit gravitational mass as a function of compactness for the EOSs listed in Table I and for three analytic solutions of Einstein's equations. The shaded region shows the prediction of Eq. (22).

Lattimer & Yahil [16] suggested that the binding energy could be approximated as

$$BE \approx 1.5 \cdot 10^{51} (M/M_{\odot})^2 \text{ ergs} = 0.084 (M/M_{\odot})^2 M_{\odot}. \quad (21)$$

This formula, in general, is accurate to $\pm 20\%$. However, a more accurate representation of the binding energy is given by [14]

$$BE/M \simeq 0.6\beta/(1 - 0.5\beta), \quad (22)$$

which incorporates some radius dependence. Thus, the observation of supernova neutrinos, and the estimate of the total radiated neutrino energy, will yield more accurate information about M/R than about M alone.

In the cases of the incompressible fluid and the Buchdahl solution, analytic results for the binding energy can be found:

$$\text{BE}_{\text{Inc}}/M = .75\beta^{-1}[(2\beta)^{-1/2} \sin^{-1} \sqrt{2\beta} - \sqrt{1-2\beta}] - 1, \quad (23)$$

$$\text{BE}_{\text{Buch}}/M = (1 - 1.5\beta)(1 - 2\beta)^{-1/2}(1 - \beta)^{-1} - 1. \quad (24)$$

These analytic results, numerical results for T VII, and the fit of Eq. (22) are compared to some recent EOSs in Fig. 5.

A new observational constraint involving I concerns pulsar glitches. Occasionally, the spin rate of a pulsar will suddenly increase (by about a part in 10^6) without warning after years of almost perfectly predictable behavior. However, Link, Epstein & Lattimer [17] argue that these glitches are not completely random: the Vela pulsar experiences a sudden spinup about every three years, before returning to its normal rate of slowing. Also, the size of a glitch seems correlated with the interval since the previous glitch, indicating that they represent self-regulating instabilities for which the star prepares over a waiting time. The angular momentum requirements of glitches in Vela imply that $\geq 1.4\%$ of the star's moment of inertia drives these events.

Glitches are thought to represent angular momentum transfer between the crust and another component of the star. In this picture, as a neutron star's crust spins down under magnetic torque, differential rotation develops between the stellar crust and this component. The more rapidly rotating component then acts as an angular momentum reservoir which occasionally exerts a spin-up torque on the crust as a consequence of an instability. A popular notion at present is that the freely spinning component is a superfluid flowing through a rigid matrix in the thin crust, the region in which dripped neutrons coexist with nuclei, of the star. As the solid portion is slowed by electromagnetic forces, the liquid continues to rotate at a constant speed, just as superfluid He continues to spin long after its container has stopped. This superfluid is usually assumed to locate in the star's crust, which thus must contain at least 1.4% of the star's moment of inertia.

The high-density boundary of the crust is located at the phase boundary between nuclei and uniform matter, where the pressure is P_t and the density is n_t . The low-density boundary is the neutron drip density, or for all practical purposes, simply the star's surface since the amount of mass between the neutron drip point and the surface is negligible. ΔR is the crust thickness: the distance between the surface and the point where $P = P_t$. One can utilize Eq. (15) to determine the moment of inertia of the crust alone using the assumptions that $P/c^2 \ll \rho$, $m(r) \simeq M$, and $\omega e^{-(\nu+\lambda)/2} \simeq \omega_R$ in the crust:

$$\Delta I \simeq \frac{8\pi}{3} \frac{\omega_R}{\Omega} \int_{R-\Delta R}^R \rho r^4 e^\lambda dr \simeq \frac{8\pi}{3\text{GM}} \frac{\omega_R}{\Omega} \int_0^{P_t} r^6 dP, \quad (25)$$

where M is the star's total mass and the TOV equation of hydrostatic equilibrium was used in the last step. The fact that the crustal EOS is of the approximate polytropic form $P \simeq K\rho^{4/3}$ can be used to approximate the integral $\int r^6 dP$. With this and Eqs. (22) and (17), the quantity $\Delta I/I$ becomes [14]

$$\frac{\Delta I}{I} \simeq \frac{28\pi P_t R^3}{3Mc^2} \frac{(1 - 1.67\beta - 0.6\beta^2)}{\beta} \left[1 + \frac{2P_t(1 + 5\beta - 14\beta^2)}{n_t m_b c^2 \beta^2} \right]^{-1}. \quad (26)$$

The EOS parameter P_t , in the units of MeV fm^{-3} , varies over the range $0.25 < P_t < 0.65$ for realistic EOSs. Like the fiducial pressure at and above nuclear density which appears in the relation Eq. (5), P_t should depend sensitively upon the behavior of the symmetry energy near nuclear density. Link, Epstein & Lattimer [17] established a lower limit to the radii of neutron stars of a given mass using Eq. (26) with P_t at its maximum value and the glitch constraint $\Delta I/I \geq 0.014$. Stellar models that are compatible with this constraint must fall to the right of the $\Delta I/I = 0.014$ contour in Fig. 1. This is equivalent to the relation

$$R > 3.9 + 3.5M/M_\odot - 0.08(M/M_\odot)^2 \text{ km}, \quad (27)$$

which is somewhat more restrictive than the one based upon causality.

I would like to thank Henryk Czyż, the local organizers and students for their gracious hospitality during the USTRON'99 meeting.

REFERENCES

- [1] A. Akmal, V.R. Pandharipande, *Phys. Rev.* **C56**, 2261 (1997).
- [2] A. Alpar, J. Shaham, *Nature* **316**, 239 (1985).
- [3] P. An, J.M. Lattimer, M. Prakash, F. Walter, (1999), to be published.
- [4] J.-P. Blaizot, J.F. Berger, J. Dechargé, M. Girod, *Nucl. Phys.* **A591**, 431 (1995).
- [5] H.A. Buchdahl, *Astrophys. J.* **147**, 310 (1967).
- [6] L. Engvik, M. Hjorth-Jensen, E. Osnes, G. Bao, E. Østgaard, *Astrophys. J.* **469**, 794 (1996).
- [7] B. Friedman, V.R. Pandharipande, *Nucl. Phys.* **A361**, 502 (1981).
- [8] N.K. Glendenning, *Phys. Rev.* **D46**, 1274 (1992).
- [9] N.K. Glendenning, S.A. Moszkowski, *Phys. Rev. Lett.* **67**, 2414 (1991).
- [10] N.K. Glendenning, J. Schaffner-Bielich, *Phys. Rev.* **C60**, 025803 (1990).

- [11] A. Golden, A. Shearer, *Astron. & Astrophys.* **342**, L5 (1999).
- [12] J.-O. Goussard, P. Haensel, J.L. Zdunik, *Astron. & Astrophys.* **330**, 1005 (1998).
- [13] H. Inoue, in *The Structure and Evolution of Neutron Stars*, ed. D. Pines, R. Tamagaki and S. Tsuruta, Redwood City, Addison Wesley, 1992, p. 63.
- [14] J.M. Lattimer, M. Prakash, 1999, in preparation.
- [15] J.M. Lattimer, M. Prakash, D. Masak, A. Yahil, *Astrophys. J.* **355**, 241 (1990).
- [16] J.M. Lattimer, A. Yahil, *Astrophys. J.* **340**, 426 (1989).
- [17] B. Link, R.I. Epstein, J.M. Lattimer, *Phys. Rev. Lett.*, Oct. 25 (1999).
- [18] H. Müller, B.D. Serot, *Nucl. Phys.* **A606**, 508 (1996).
- [19] H. Muther, M. Prakash, T.L. Ainsworth, *Phys. Lett.* **199**, 469 (1987).
- [20] J.A. Orosz, E. Kuulkers, *Mon. Not. Royal Ast. Soc.* **305**, 132 (1999).
- [21] V. Osherovich, L. Titarchuk, *Astrophys. J. Lett.* **522**, L113 (1999).
- [22] D. Page, *Astrophys. J.* **442**, 273 (1995).
- [23] J.M. Pearson, *Phys. Lett.* **B271**, 12 (1991).
- [24] M. Prakash, T.L. Ainsworth, J.M. Lattimer, *Phys. Rev. Lett.* **61**, 2518 (1988).
- [25] M. Prakash, I. Bombaci, M. Prakash, J.M. Lattimer, P.J. Ellis, R. Knorren, *Phys. Rep.* **280**, 1 (1997).
- [26] M. Prakash, J.R. Cooke, J.M. Lattimer, *Phys. Rev.* **D52**, 661 (1995).
- [27] C.E. Rhoades, R. Ruffini, *Phys. Rev. Lett.* **32**, 324 (1974).
- [28] R.W. Romani, *Astrophys. J.* **313**, 718 (1987).
- [29] R. Rutledge, L. Bildstein, E. Brown, G.G. Pavlov, V.E. Zavlin, AAS Meeting #193, Abstract #112.03.
- [30] N.S. Shulz, *Astrophys. J.* **511**, 304 (1999).
- [31] L. Stella, M. Vietra, *Phys. Rev. Lett.* **82**, 17 (1999).
- [32] L. Stella, M. Vietra, S. Morsink, *Astrophys. J. Lett.* **524**, L63 (1999).
- [33] D. Stickland, C. Lloyd, A. Radzuin-Woodham, *Mon. Not. Royal Ast. Soc.* **286**, L21 (1997).
- [34] S.E. Thorsett, D. Chakrabarty, *Astrophys. J.* **512**, 288 (1998).
- [35] L. Titarchuk, *Astrophys. J.* **429**, 340 (1994).
- [36] R.C. Tolman, *Phys. Rev.* **55**, 364 (1939).
- [37] J.H. van Kerkwijk, J. van Paradijs, E.J. Zuiderwijk, *Astron. & Astrophys.* **303**, 497 (1995).
- [38] F. Walter, S. Wolk, R. Neuhaüser, *Nature* **379**, 233 (1996).
- [39] F. Walter, L.D. Matthews, *Nature* **389**, 358 (1997).
- [40] R.B. Wiringa, V. Fiks, A. Fabrocine, *Phys. Rev.* **C38**, 1010 (1988).
- [41] D.H. Youngblood, H.L. Clark, Y.-W. Lui, *Phys. Rev. Lett.* **82**, 691 (1999).